Optical Properties of *c*-Axis Oriented Superconducting MgB_2 Films

J. J. Tu,[1,*] G. L. Carr,[2] V. Perebeinos,[1] C. C. Homes,[1] M. Strongin,[1] P. B. Allen,[3] W. N. Kang,[4] Eun-Mi Choi,[4] Hyeong-Jin Kim,[4] and Sung-Ik Lee[4]

[1]*Department of Physics, Brookhaven National Laboratory, Upton, New York 11973-5000*
[2]*NSLS, Brookhaven National Laboratory, Upton, New York 11973-5000*
[3]*Department of Physics and Astronomy, SUNY Stony Brook, Stony Brook, New York 11794-3800*
[4]*National Creative Research Initiative Center for Superconductivity, Department of Physics, Pohang University of Science and Technology, Pohang 790-784, Korea*
(Received 2 July 2001; published 11 December 2001)

Temperature dependent optical conductivities and dc resistivity of *c*-axis oriented superconducting ($T_c = 39.6$ K) MgB_2 films (~450 nm) have been measured. The normal state *ab*-plane optical conductivities can be described by the Drude model with a temperature independent Drude plasma frequency of $\omega_{p,D} = 13\,600 \pm 100\ \text{cm}^{-1}$ or 1.68 ± 0.01 eV. The normal state resistivity is fitted by the Bloch-Grüneisen formula with an electron-phonon coupling constant $\lambda_{\text{tr}} = 0.13 \pm 0.02$. The optical conductivity spectra below T_c of these films suggest that MgB_2 is a multigap superconductor.

DOI: 10.1103/PhysRevLett.87.277001 PACS numbers: 74.25.Gz, 74.25.Kc, 74.76.Db

The recent discovery of superconductivity in MgB_2 with T_c of 39 K has generated much scientific interest [1]. As in the case of the high-T_c cuprates, debate rages as to the mechanism of superconductivity in this material. Initial isotope effect measurements suggested electron-phonon coupling as the pairing mechanism for superconductivity in MgB_2 [2,3]. Many theoretical studies [4–7] since then have concluded that strong electron-phonon coupling is responsible for the high transition temperature, with $\lambda \sim 1$. However, other pairing mechanisms have also been proposed, e.g., "dressing" and "undressing" of holes [8], acoustic plasmons [9], and the "filamentary" thoery [10]. This inconclusive state of affairs is mainly due to the lack of consensus on many important physical quantities in MgB_2. For example, the reported values for the superconducting gap 2Δ vary from 4 meV [11] to 14 meV [12]. Infrared spectroscopy is able to measure such quantities as the scattering rate $1/\tau$, the Drude plasma frequency $\omega_{p,D}$, and 2Δ [13]. In this work, we analyze the optical data of MgB_2 to determine the electron-phonon coupling constant, λ_{tr}, in a similar fashion as in the optical study [14] of $Ba_{0.6}K_{0.4}BiO_3$ ($T_c \sim 30$ K), where $\lambda_{\text{tr}} \sim 0.2$ was obtained experimentally.

There have been very few optical studies on MgB_2 until now. Gorshunov *et al.* [15] measured the reflectance of a polycrystalline pellet using the grazing angle method. Pronin *et al.* [16] examined the complex optical conductivity of a MgB_2 thin film in the frequency range of 0.5–4 meV. More recently, Jung *et al.* [17] carried out transmission measurements on a *c*-axis oriented MgB_2 film (~50 nm) with $T_c \sim 33$ K. However, to obtain the optical constants of bulk MgB_2 in a wide frequency region, reflectivity measurements are the preferred method.

In this Letter, temperature dependent optical conductivities and dc resistivity of *c*-axis oriented superconducting ($T_c = 39.6$ K) MgB_2 films (~450 nm) are reported. The normal state *ab*-plane optical conductivities can be well described by the Drude model with $\omega_{p,D} = 13\,600 \pm 100\ \text{cm}^{-1}$. Using this plasma frequency $\lambda_{\text{tr}} = 0.13 \pm 0.02$ is determined by fitting the dc resistivity data. In addition, the optical conductivities in the superconducting state exhibit complex behavior suggesting that MgB_2 is a multigap superconductor.

For this study, several *c*-axis oriented MgB_2 films are used: one very thin film (~50 nm) similar to the film studied by Jung *et al.* [17] and two thicker films (~450 nm). These high-quality *c*-axis oriented films were deposited on *c*-cut Al_2O_3 substrates using a pulsed laser deposition method as described previously [18]. These MgB_2 films have a tan appearance, similar to the high purity MgB_2 polycrystalline samples [2]. The thick MgB_2 films (~450 nm) are opaque in the visible region. Temperature dependent reflectance is measured in a near-normal-incidence arrangement from ~30 to over $22\,000\ \text{cm}^{-1}$, with the electric field parallel to the *ab*-plane on Bruker IFS 66v/S and 113v spectrometers. The absolute reflectance is determined by evaporating a gold film *in situ* in ultrahigh vacuum (~10^{-8} Torr). The details of this technique have been described previously [19].

In Fig. 1(a), the dc sheet resistance $R_\square$ versus temperature, measured by a standard four-probe technique of a MgB_2 film (~450 nm), is shown. The low temperature region near $T_c = 39.6$ K is given in the inset. The superconducting transition in this film is extremely sharp with a transition region of $\delta T_c < 0.1$ K indicating that these thick MgB_2 films are of excellent quality [18].

The raw data of the optical measurements on these MgB_2 films (~450 nm) are summarized in Fig. 2. Several sharp phonon features can be clearly identified in Fig. 2(a). As a comparison, the reflectance of the thin MgB_2 film (~50 nm) is also measured. The two strong infrared active TO phonons of *c*-cut Al_2O_3 crystals at 440 and 570 cm^{-1} [20] can be easily observed for the thin MgB_2 film but completely absent for the thick films (~450 nm), indicating

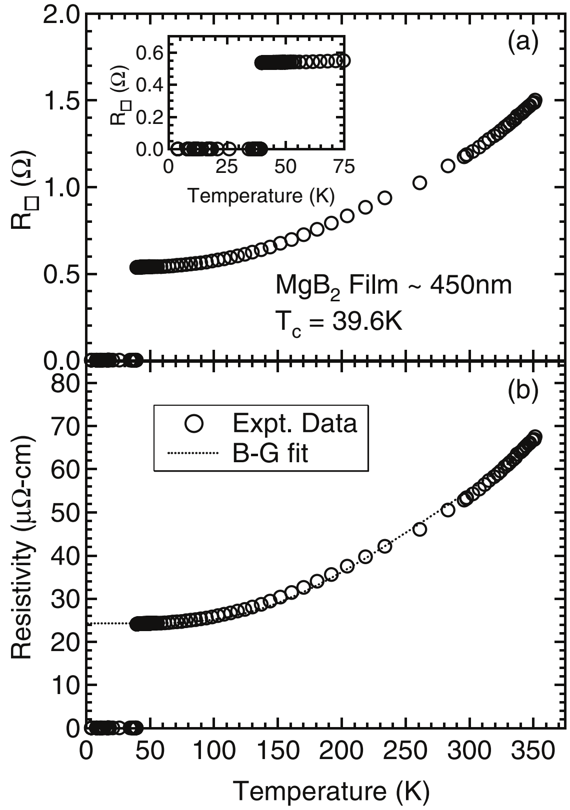

FIG. 1. The dc resistivity data of a c-axis oriented MgB_2 film ($t \sim 450$ nm). (a) Temperature dependent $R_\square$ (open circles). Inset: Low temperature region of $R_\square$ near T_c. (b) Temperature dependence of the resistivity together with a fit to the Bloch-Grüneisen formula (dotted line).

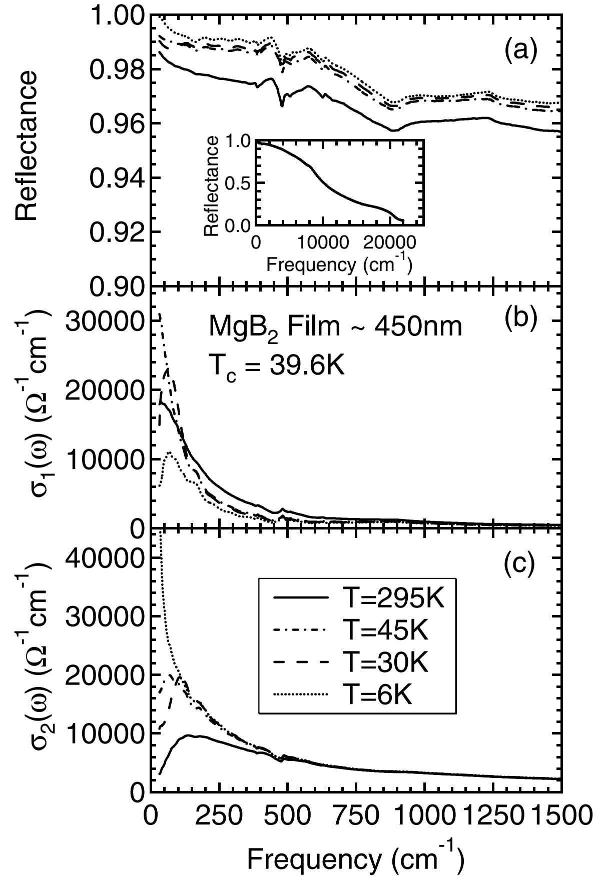

FIG. 2. The temperature dependent ab-plane optical data of c-axis oriented MgB_2 films ($t \sim 450$ nm) from 30 to 1500 cm^{-1}. (a) The reflectance data showing sharp phonon modes. Inset: Optical reflectance spectrum for the entire frequency region at 295 K. (b) Temperature dependent $\sigma_1(\omega)$. (c) Temperature dependent $\sigma_2(\omega)$.

that the optical properties measured for these thick MgB_2 films (~450 nm) are intrinsic. In the inset, the reflectance data at 295 K is given for the entire frequency region: from 30 to 22 000 cm^{-1}. The results of a Kramers-Kronig analysis are shown as temperature dependent $\sigma_1(\omega)$ in Fig. 2(b) and $\sigma_2(\omega)$ in Fig. 2(c). Superconducting behavior can be easily identified as a drop in $\sigma_1(\omega)$ at low frequencies below T_c.

The normal state optical conductivities of these MgB_2 films are analyzed in Fig. 3. The low frequency optical conductivities can be well described by the Drude model:

$$\tilde{\sigma}(\omega) = \sigma_1 + i\sigma_2 = \frac{1}{4\pi}\frac{\omega_{p,D}^2 \tau}{1 - i\omega\tau}, \qquad \omega_{p,D}^2 = \frac{4\pi n e^2}{m^*}, \tag{1}$$

where $\omega_{p,D}$ is the Drude plasma frequency, $1/\tau$ is the scattering rate, n is the number of free carriers per unit volume, and m^* is the average effective mass of the occupied carrier states. The Drude model describes the experimental data surprisingly well at 295 K as shown in Fig. 3(a) with the parameters $\omega_{p,D} = 13\,600 \pm 100\ cm^{-1}$ and $1/\tau = 170 \pm 5\ cm^{-1}$. This Drude plasma frequency of 13 600 cm^{-1} is quite consistent with the value obtained from an optical study of a polycrystalline MgB_2 sample [21]. However, in addition to the Drude peak, some other contributions to $\sigma_1(\omega)$ are also observed in that optical study [21]. Using the optical data, one can determine the dc resistivity $\rho = 1/\sigma_0 = 53 \pm 2\ \mu\Omega$ cm at 295 K, as well as the averaged thickness of this MgB_2 film $t = \rho/R_\square = 450 \pm 20$ nm which agrees very well with the typical thickness of 400 nm of these films [18]. It is interesting that the experimental Drude plasma frequency of 1.68 eV is much smaller than the value of ~7 eV predicted by calculations of the electronic structure in MgB_2 [4–7]. These calculations usually give values of Drude plasma frequencies that are reasonably close to experimental values [22].

Keeping $\omega_{p,D}$ the same, the optical conductivities at 45 K as given in Fig. 3(b) can again be well fitted with the Drude model with a scattering rate of $1/\tau = 75 \pm 5\ cm^{-1}$. In addition, the dc resistivity at 45 K is in good agreement with the zero frequency extrapolation of $\sigma_1(\omega)$. Therefore, the dc resistivity and the optical conductivity are in excellent agreement.

From the ab-plane optical data, one can calculate the frequency dependent electron-phonon coupling constant $\lambda(\omega)$ in the extended Drude formalism [23]:

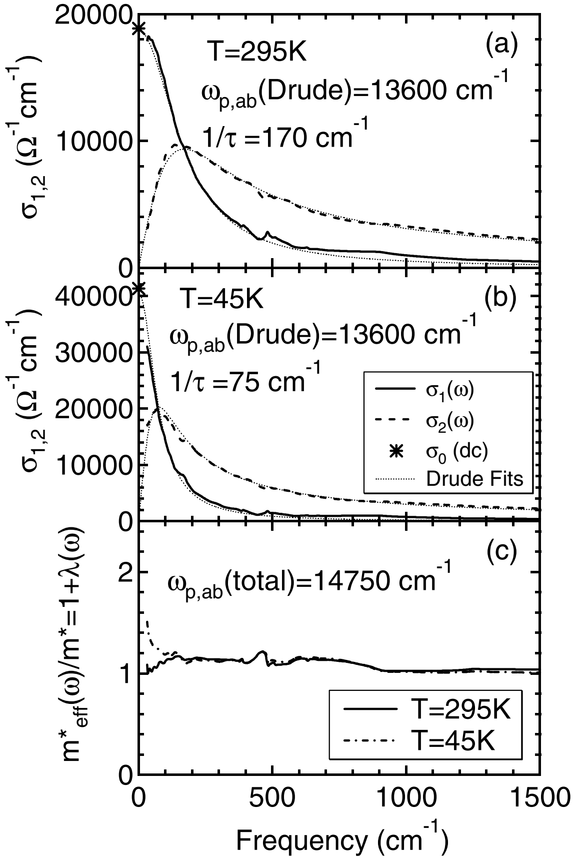

FIG. 3. The analysis of normal state *ab*-plane optical constants of the *c*-axis oriented MgB_2 films. (a) Frequency dependent optical conductivities: $\sigma_1(\omega)$ and $\sigma_2(\omega)$ at 295 K (thick lines) with the Drude fits (thin dotted lines). (b) Frequency dependent optical conductivities at 45 K. (c) Frequency dependent effective mass ratio for $T > T_c$.

$$\frac{m^*_{\text{eff}}(\omega)}{m^*} = 1 + \lambda(\omega) = \frac{1}{4\pi}\frac{\omega_p^2}{\omega}\,\text{Im}\left[\frac{1}{\tilde{\sigma}(\omega)}\right], \qquad (2)$$

where ω_p is the total plasma frequency. The result of this analysis is shown in Fig. 3(c). The value of $\lambda(\omega)$ derived optically varies from 0 to about 0.2, where $\omega_p = 14\,750 \pm 150\ \text{cm}^{-1}$ is derived from the conductivity sum rule. The value of ω_p is slightly larger than $\omega_{p,D}$ due to the fact that the sum rule captures additional spectral weight in the high frequency region.

The transport electron-phonon coupling constant λ_{tr} is traditionally determined from the temperature dependent dc resistivity using the Bloch-Grüneisen formula,

$$\rho(T) = \rho_0 + \lambda_{\text{tr}}\frac{4\pi}{\omega_{p,D}^2}\frac{128\pi(k_BT)^5}{(k_B\Theta_D)^4}\int_0^{\Theta_D/2T}\frac{x^5}{\sinh^2 x}\,dx\,, \qquad (3)$$

with three parameters: ρ_0—the residual resistivity at $T = 0$; Θ_D—the Debye temperature; and λ_{tr}. A nonlinear least squares fit to the resistivity data with Eq. (3) is given in Fig. 1(b) using $\omega_{p,D} = 1.68 \pm 0.01$ eV. The experimental curve and the theoretical fit agree quite well with the fitting parameters: $\rho_0 = 24.3 \pm 0.3\ \mu\Omega$ cm; $\Theta_D = 950 \pm 100$ K; and $\lambda_{\text{tr}} = 0.13 \pm 0.02$. The value $\Theta_D = 950 \pm 100$ K is consistent with the experimentally measured value that varies from 800 K [24] to 1050 K [25]. However, $\lambda_{\text{tr}} = 0.13 \pm 0.02$ is significantly smaller than most theoretical predictions of $\lambda \sim 1$ [4–7] in MgB_2.

The optical conductivities of these MgB_2 films in the superconducting state are examined in Fig. 4. The superfluid plasma frequency is found to be $\omega_{p,S} = 7300 \pm 50\ \text{cm}^{-1}$ at 6 K from the Ferrel-Glover-Tinkham (FGT) sum rule. However, the optical spectra below T_c cannot be fitted by the BCS model using a single isotropic gap. An attempt to fit the optical data at 30 and 6 K using a BCS model [26] is shown in Figs. 4(a) and 4(b) with the parameters $2\Delta = 65\ \text{cm}^{-1}$ and $1/\tau = 75\ \text{cm}^{-1}$. There are significant deviations between the experimental data and the BCS calculations. The complex gap behavior observed in our data adds support to the suggestion that MgB_2 is a multigap superconductor [5,12,25].

Four sharp phonon peaks are identified in $\sigma_1(\omega)$, as shown in Fig. 4(c), that can be assigned to Γ-point optical phonons in MgB_2 [4]. The two strong phonon peaks

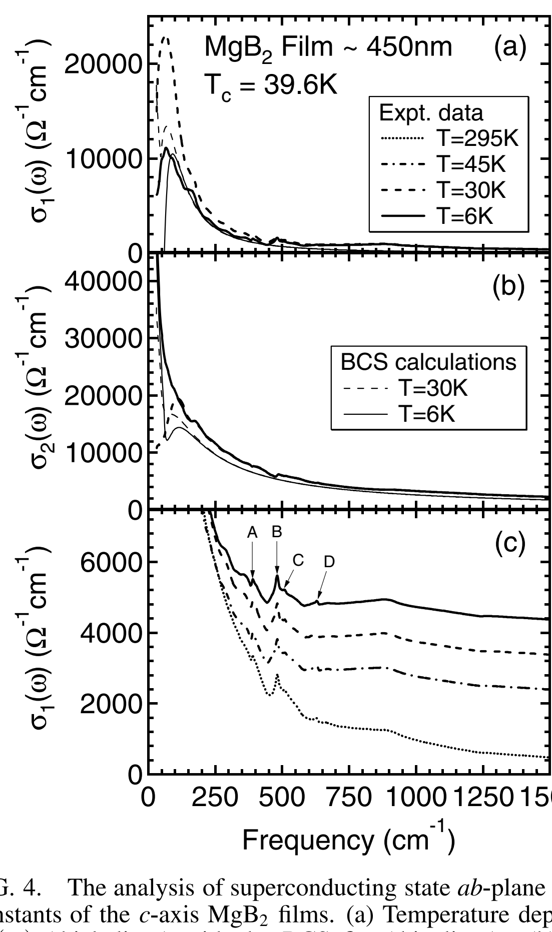

FIG. 4. The analysis of superconducting state *ab*-plane optical constants of the *c*-axis MgB_2 films. (a) Temperature dependent $\sigma_1(\omega)$ (thick lines) with the BCS fits (thin lines). (b) Temperature dependent $\sigma_2(\omega)$ (thick lines) with the BCS fits (thin lines). (c) Temperature dependent $\sigma_1(\omega)$ showing four Γ-point phonons. The spectra corresponding to different temperatures are offset for clarity.

marked as A and B are the two infrared active lattice modes: at 380 cm^{-1} (E_{1u}) and at 480 cm^{-1} (A_{2u}). Their relatively large oscillator strengths are the consequence of the low plasma frequency in MgB_2. Two weak phonon peaks marked as C and D at 510 and 630 cm^{-1} are tentatively assigned as the Raman active E_{2g} mode and the silent B_{1g} mode [4]. These two even phonons become infrared active maybe because of the lattice imperfections in the films. Alternatively, several Raman studies [27] on MgB_2 have assigned a broadband centered at 620 cm^{-1} as the E_{2g} mode. None of the four sharp phonon modes exhibit detectable changes in either their intensities, peak positions, or linewidths going through T_c.

The surprising aspect of our results is the small value of $\lambda_{tr} = 0.13$ in MgB_2. Until now, the McMillan and the Allen-Dynes treatments of the BCS theory [28] have been used almost universally for MgB_2. However, a simple application of these results [28] with $\lambda \cong \lambda_{tr} = 0.13$ will give $T_c < 1$ K which suggests that the conventional BCS theory [28] cannot describe the value of T_c in MgB_2 without major modifications. On the other hand, electron-phonon coupling may still be the pairing mechanism for MgB_2 in an unconventional way: (i) the superconducting gap in MgB_2 has unusual properties. Gap anisotropy [29] modifies T_c relative to the McMillan formula; (ii) the λ value that goes into the McMillan formula can differ with respect to λ_{tr} [30]. The possibility of λ being much larger than λ_{tr} for MgB_2 should be considered; (iii) c-axis optical and transport properties should be experimentally studied to explore any anisotropic effects. In addition to the electron-phonon mechanism, given the small value of $\lambda_{tr} = 0.13$ other mechanisms of superconductivity in MgB_2 should also be investigated. It is interesting to note that many of the optical constants in MgB_2 are quite similar to those in $Ba_{0.6}K_{0.4}BiO_3$ [14], e.g., the scattering rate, the Drude plasma frequency, and particularly the small value of λ_{tr}. A common mechanism might be responsible for superconductivity in both systems. Furthermore, having a small free carrier plasma frequency (<3 eV) seems to be a universal characteristic shared by almost all superconductors with a $T_c > 30$ K which means that the issue of reduced screening should be treated carefully in all of these systems.

In conclusion, we have measured optical conductivities and dc resistivity of c-axis oriented superconducting MgB_2 films. The small measured λ_{tr} value is a puzzle and poses a serious problem to the conventional strong electron-phonon coupling picture. Other theoretical models need to be explored to account both for the complex behavior of the superconducting gap and the possibility of a different pairing mechanism in MgB_2.

We thank P.C. Canfield, V.J. Emery, J.E. Hirsch, P.D. Johnson, S.A. Kivelson, T. Valla, and T. Vogt for helpful discussions. Part of the work was supported by the U.S. Department of Energy under Contract No. DE-AC02-98CH10886 and the other part by the Ministry of Science and Technology of Korea through the Creative Research Initiative Program.

*Electronic address: jtu@bnl.gov

[1] J. Nagamatsu *et al.,* Nature (London) **410**, 63 (2001).
[2] S.L. Bud'ko *et al.,* Phys. Rev. Lett. **86**, 1877 (2001).
[3] D.G. Hinks, H. Claus, and J.D. Jorgensen, Nature (London) **411**, 457 (2001).
[4] J. Kortus *et al.,* Phys. Rev. Lett. **86**, 4656 (2001).
[5] A.Y. Liu, I.I. Mazin, and J. Kortus, Phys. Rev. Lett. **87**, 087005 (2001).
[6] Y. Kong, O.V. Dolgov, O. Jepsen, and O.K. Anderson, Phys. Rev. B **64**, 020501(R) (2001).
[7] J.M. An and W.E. Pickett, Phys. Rev. Lett. **86**, 4366 (2001).
[8] J.E. Hirsch and F. Marsiglio, cond-mat/0102479.
[9] K. Voelker, V.I. Anisimov, and T.M. Rice, cond-mat/0103082.
[10] J.C. Phillips and J. Jung, cond-mat/0102261.
[11] G. Rubio-Bollinger, H. Suderow, and S. Vieira, Phys. Rev. Lett. **86**, 5582 (2001).
[12] P. Szabó *et al.,* Phys. Rev. Lett. **87**, 137005 (2001).
[13] M. Tinkham, *Introduction to Superconductivity* (Krieger, Malabar, Florida, 1975); B. Farnworth *et al.,* Phys. Rev. B **10**, 5119 (1976); F. Gao *et al.,* Phys. Rev. B **54**, 700 (1996).
[14] A.V. Puchkov, T. Timusk, W.D. Mosley, and R.N. Shelton, Phys. Rev. B **50**, 4144 (1994).
[15] B. Gorshunov *et al.,* Eur. Phys. J. B **21**, 159 (2001).
[16] A.V. Pronin, A. Pimenov, A. Loidl, and S.I. Kransnosvobodtsev, Phys. Rev. Lett. **87**, 097003 (2001).
[17] J.H. Jung *et al.,* cond-mat/0105180.
[18] W.N. Kang *et al.,* Science **292**, 1521 (2001).
[19] C.C. Homes, M. Reedyk, D. Crandles, and T. Timusk, Appl. Opt. **32**, 2972 (1993).
[20] A.S. Barker, Phys. Rev. **132**, 1474 (1963).
[21] A.B. Kuz'menko *et al.,* cond-mat/0107092.
[22] W.E. Pickett, P.B. Allen, and H. Krakauer, Phys. Rev. B **37**, 7482 (1988).
[23] A.V. Puchkov, D.N. Basov, and T. Timusk, J. Phys. C **8**, 10 049 (1996).
[24] R.K. Kremer, B.J. Gibson, and K. Ahn, cond-mat/0102432.
[25] F. Bouquet *et al.,* Phys. Rev. Lett. **87**, 047001 (2001).
[26] W. Zimmermann *et al.,* Physica (Amsterdam) **183C**, 99 (1991).
[27] X.K. Chen *et al.,* cond-mat/0104005; A.F. Goncharov *et al.,* cond-mat/0104042; J. Hlinka *et al.,* cond-mat/0105275.
[28] W.L. McMillan, Phys. Rev. **167**, 331 (1968); P.B. Allen and R.C. Dynes, Phys. Rev. B **12**, 905 (1975).
[29] P.B. Allen, Z. Phys. B **47**, 45 (1982), and references therein.
[30] P.B. Allen, in *Handbook of Superconductivity,* edited by C.P. Poole (Academic, San Diego, 2000), p. 478.